Green World Journal
ISSN: 2737-6109

CaMeRa Editorial

ARTICLE

Kinematic control of a vehicle via a GPS sensor for autonomous driving

Danny Zea

Escuela Superior Politécnica de Chimborazo, Sede Orellana, El Coca EC220001, Ecuador

Correspondence: danny.zea@espoch.edu.ec + 593 97 907 1851

DOI/URL: https://doi.org/10.53313/gwj42023

Abstract: The research analyzes the behavior and performance of a control law that has been validated in a previous study in a 3D simulation program. Now, it will be evaluated in a Mazda 6 vehicle with the objective of driving along a previously designed trajectory. This is possible thanks to the use of a GPS sensor as well as additional sensors that allow to know the direct kinematics of the vehicle at each instant of time. Experimental tests were carried out with the use of a Raspberry pi 3 b+ which is responsible for receiving the information from the sensors and then processed this information so that the control law allows sending the control actions to the actuators. Finally, the results are presented in order to be used for future research that will allow the implementation of a fully autonomous driving system.

Keywords: Kinematic control, GPS sensor, Autonomous driving

Check for updates

Cite: Zea, D. (2021). Kinematic control of a vehicle via a GPS sensor for autonomous driving. Green World Journal, 04(02), 23. https://doi.org/10.53313/gwj42023

Received: 26/July/2021

Accepted: 28/August/2021

Published: 31/August/2021

Prof. Carlos Mestanza-Ramón, PhD.
Editor-in-Chief / CaMeRa Editorial
editor@greenworldjournal.com

1. Introduction

For decades, the Global Positioning System GPS has allowed the triangulation of countless objects on the planet Earth, triggering the proliferation of several applications. Autonomous driving systems in the last decade have had an important role and have been one of the main research topics, especially focused on the reliability when interacting with the environment, even more so when there are several static and dynamic objects involved in real traffic [1]. One of the relevant points when talking about reliability, are the sensors, and specifically the GPS sensor that allows knowing the location at every instant of time, but many times it is affected by interference when passing through closed places such as infrastructure of considerable heights that weaken the reception and on repeated occasions the signal can be lost [2]; causing the vehicle to lose information about its location [3-4]. The development of more robust GPS sensors with better techniques to improve their accuracy is booming, especially for applications in autonomous driving. However, when the GPS signal is affected, the fusion of sensors such as a LIDAR, 3D vision camera, etc., comes into play to compensate for vehicle disorientation and avoid accidents on the road [5][6].

Among a diversity of GPS sensors that exist today in the market that offer different performances, most of them are limited at the time of acquiring them because of their high economic value and hindering research in research groups [7]. An alternative is to use 3D simulation programs that allow shortening research times and through emulation validate proposals for applications in autonomous driving before taking them to the real world [8-9]. In this article, we evaluate the proposal developed in previous research that was carried out in a Webots 3D simulation program and that will now be tested in a Mazda 6 vehicle with an electromechanical system that allows to take action on the vehicle. The proposal proposes a control law for tracking the vehicle in a desired trajectory previously defined through a GPS sensor, then the performance of the GPS sensor is validated by analyzing its accuracy error when the vehicle travels over the trajectory. It is important to highlight that the control law does not consider obstacles on the road nor does it allow the vehicle to interact with its environment, for this reason the tests are performed on a track for driving applications located at the Rumiñahui Institute, Pichincha Province, Ecuador. In addition, the experimental tests are conducted with a driver inside the vehicle, with the objective of taking control of the vehicle when an emergency arises and above all the driver has an emergency button that allows to turn off and disconnect the entire system.

This research is divided into 5 sections. Section 1 is the Introduction; section 2 explains the design of the controller and the control law. Then, section 3 describes the system structure with the description of each of the blocks. Section 4 shows the scenario where the experimental tests are performed and the characteristics of the vehicle. Section 5 presents the results of the vehicle behavior with the GPS sensor. Finally, section 7 presents the conclusions.

2. Kinematic design of the controller

The kinematics of the controller starts from the simplified kinematic model, which uses Ackerman steering at the front wheels and creates a center of rotation at some point along the axis of the rear wheels[10]. Figure 1. illustrates the simplified kinematic model.

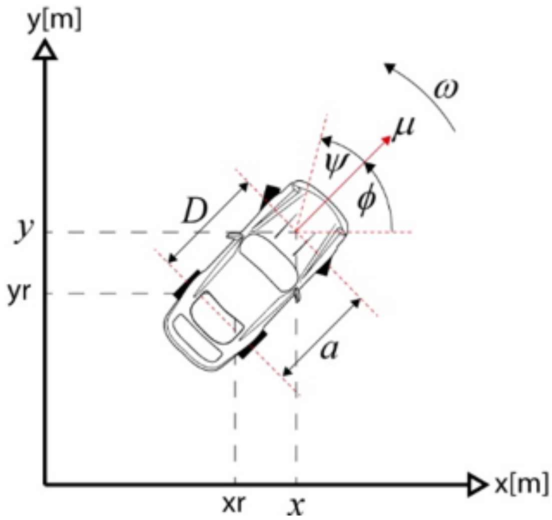

Figure 1. Geometric Model of a car-like robot

The kinematics of the controller starts from the simplified kinematic model, which uses Ackerman steering at the front wheels and creates a center of rotation at some point along the axis of the rear wheels [10]. Figure 1. illustrates the simplified kinematic model.

The kinematic model configuration is defined by the following equation:

$$\begin{bmatrix} \dot{x} \\ \dot{y} \\ \dot{\phi} \end{bmatrix} = \begin{bmatrix} \cos(\phi) & -a\sin(\phi) \\ \sin(\phi) & a\cos(\phi) \\ 0 & 1 \end{bmatrix} \begin{bmatrix} \mu \\ \omega \end{bmatrix} \quad (1)$$

The compact form of writing equation (2) is defined by:

$$\dot{\mathbf{h}}(t) = \mathbf{J}(\phi)\mathbf{v}(t) \quad (2)$$

Therefore, $\dot{\mathbf{h}}(t) = [\dot{x} \quad \dot{y}]^T \in R^2$, represents the vector of Cartesian velocities at some point of interest defined by the distance a; $\mathbf{J}(\phi) \in R^{2x2}$ defines the Jacobian matrix and $\mathbf{v}(t) = [\mu \quad \omega]^T$ is the vector of control and maneuverability with and as the angular and linear velocity of the car-like vehicle respectively. The angle of the front wheels sets the direction the vehicle takes and is defined by:

$$\psi = \tan^{-1}\left(\frac{D\omega}{\mu}\right) \quad (6)$$

The controller design starts from the simplified kinematic model defined in equation (2), where the control vector is defined by:

$$\mathbf{v_c}(t) = \mathbf{J}^{-1}(\phi)\dot{\mathbf{h}}(t) \quad (7)$$

Equation (4) defines the control law that allows the vehicle to adjust its motion to follow a previously configured trajectory. Therefore, $\mathbf{J}^{-1}(\phi)$ it represents the inverse Jacobian matrix $\dot{\mathbf{h}}(t) = [\dot{x}_d \quad \dot{y}_d]^T$, it is the vector of velocities and will now be defined by $\dot{\mathbf{h}}_d(t) = [\dot{x}_d \quad \dot{y}_d]^T$ as the vector of desired velocities, then a new parameter $\tilde{\mathbf{h}} = \mathbf{h_d} - \mathbf{h}$ is defined that allows quantifying the position error, where $\mathbf{h}_d$ it represents the desired position vector and $\mathbf{h}$ the current position of the vehicle. Finally, the control law is defined in equation (5), where $\mathbf{K_1}$ is a diagonal matrix that allows to compensate the position error $\mathbf{K}_2$ and is a diagonal matrix that allows to fine tune the control actions.

$$\mathbf{v_c}(t) = \mathbf{J}^{-1}(\phi)\left(\dot{\mathbf{h}}_\mathbf{d}(t) + \mathbf{K_2}\tanh\left(\mathbf{K_2}^{-1}\mathbf{K_1}\tilde{\mathbf{h}}(t)\right)\right) \quad (5)$$

3. System structure

The full-scale implementation of the proposal, where the control law can be validated in the real world, is possible thanks to the configuration illustrated in figure 2, with the following blocks: (i) Mazda 6, is a conventional vehicle that has been instrumented with an electromechanical system to take control over the steering wheel, accelerator and brake, it also has sensors such as a GPS and a compass that allow to know its position and orientation, on the other hand are the sensors for reading about its speed and position of the steering wheel at every instant of time; ii) Raspberry pi 3 b+, is a low-cost small board computer, being in charge of reading the input signals from the sensors that will be processed to perform control actions through the actuators and iii) Power stage, is the block in charge of isolating and amplifying the output signals from the computer to the actuators.

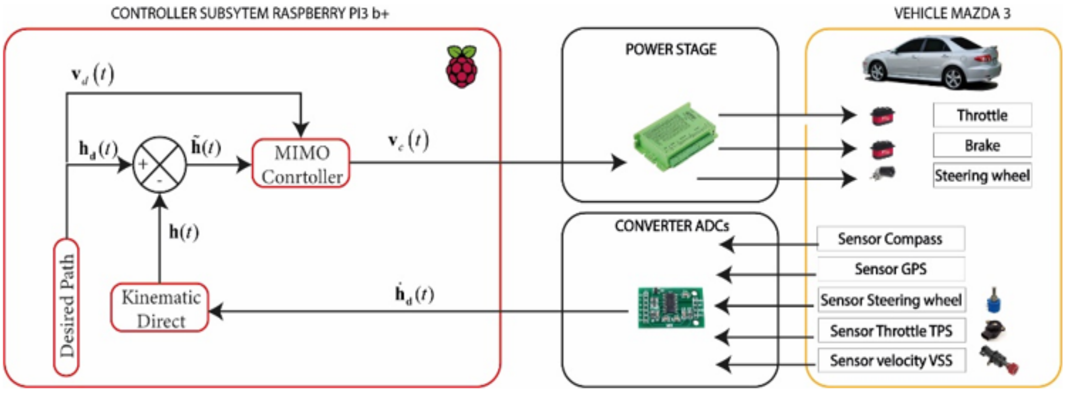

Figure 2. Driving structure

4. Scenario

An important point to validate the proposal is the consideration that the vehicle does not have an obstacle avoidance system and will not be able to interact with pedestrians or other vehicles, for which it will be validated in a suitable scenario for autonomous driving tests at the Rumiñahui Institute in the province of Pichincha. The dimensions of the scenario are 177 meters long and 60 meters wide. The scenario is illustrated in figure3.

Figure 3. Experimental Scenario

4.1 Mazda 6 vehicle

The vehicle is a 2008 Mazda 6 model, which has an electromechanical system for the actuators and sensors. The control actions are sent to three servomotors that control the accelerator, brake and steering wheel respectively; while four sensors are read to know the position of the steering wheel with a potentiometer of ten turns, the TPS sensor (Throttle Position Sensor) to know the position of the accelerator, the VSS sensor (Vehicle Speed Sensor) to read the vehicle speed, the compass sensor to know the vehicle orientation and finally the GPS sensor to know the vehicle location. The input signals are read through a digital and analog I/O module that allows the parameterization and sending to a Raspberry Pi 3 b+ to process these signals and then be sent to a power module to control the servomotors. Figure 4. Illustrates the Mazda 6 vehicle.

Figure 4. Mazda 6 vehicle

5. Results and discussion

After making some adjustments and testing the controller on the Mazda 6 vehicle, the control law (5) is established with the following parameters: the desired route is defined by $\tilde{\mathbf{h}}_d(t) = [0.1t \quad 0.5\sin(0.1t)][m]$ with the respective transformation of the geodesic coordinates to Cartesian coordinates in order to facilitate the calculations in the controller, gain matrices $\mathbf{K}_1 = diag[0.52 \quad 0.6]$ and $\mathbf{K}_2 = diag[0.9 \quad 0.92]$. The initial starting points of the vehicle are: $\mathbf{p}(0) = [27 \quad -14 \quad -1.12]^T[m]$.

The sensors are installed in the trunk of the vehicle at the height of the axle of the rear wheels and from this point the control point is established $a = 2.725[m]$. The sampling time set for the controller on the Raspberry pi 3 b+ is of $100[s]$ with total vehicle travel time of $30[s]$. The characteristics of the Mazda 6 vehicle are listed in Table 1:

Table 1. Performance, dimensions, weight and capacities

Prestaciones, dimensiones, peso y capacidades	
Top speed	214 km/h
Acceleration 0-100 km/h	9,9 s
Type of bodywork	Turismo
Number of doors	4
Length	4.735 mm
Width	1.795 mm
Height	1.440 mm
Wheelbase	2.725 mm
Front track	1.550 mm

Rear track	1.550 mm
Weight	1.370 kg
Combustion Engine	
Purpose	Vehicle drive
Fuel	Gasoline
Maximum power	147 CV / 108 kW
Revolutions maximum power	6.500 rpm
Maximum torque	184 Nm
Revolutions at maximum torque	4.000 rpm
Location	Transverse front
Number of cylinders	4
Cylinder arrangement	Online
Displacement	1.999 cm^3
Compression ratio	10 a 1
Transmission	
Drive	Front
Gearbox	Automatic
Number of gears	6

The characteristics of the sensors used in the instrumentation of the Mazda 6 vehicle are illustrated in Table 2.

Table 2. Sensors equipped in the vehicle.

Position on the vehicle	Sensor	Model	Specifications/Inputs	Values
sensors slot rear	GPS	ProPak-V3TM	Horizontal position accuracy	0.35 m
			Resolution	0.04 m
			Speed Resolution	0.03 m/s
			Velocity maximum	515 m/s
sensors slot rear	Compass	NEO-M8T	xAxis	True
			yAxis	True
			zAxis	True
			Resolution	5 milli-gauss
vehicle steering wheel	Potentiometry	3590S-2-103L	Resistance Range:	10 kOhm
			Standard Tolerance	+ / - 5%
			Linearity	0,20 %
			Power	2 Watts
			Number of Turns	10
			Shaft Diameter	6,35mm

The path of the vehicle along the previously desired trajectory is illustrated in figure 4 and shows the Cartesian positions of the vehicle $\tilde{\mathbf{h}}$ as it travels along the desired trajectory $\tilde{\mathbf{h}}_d$.

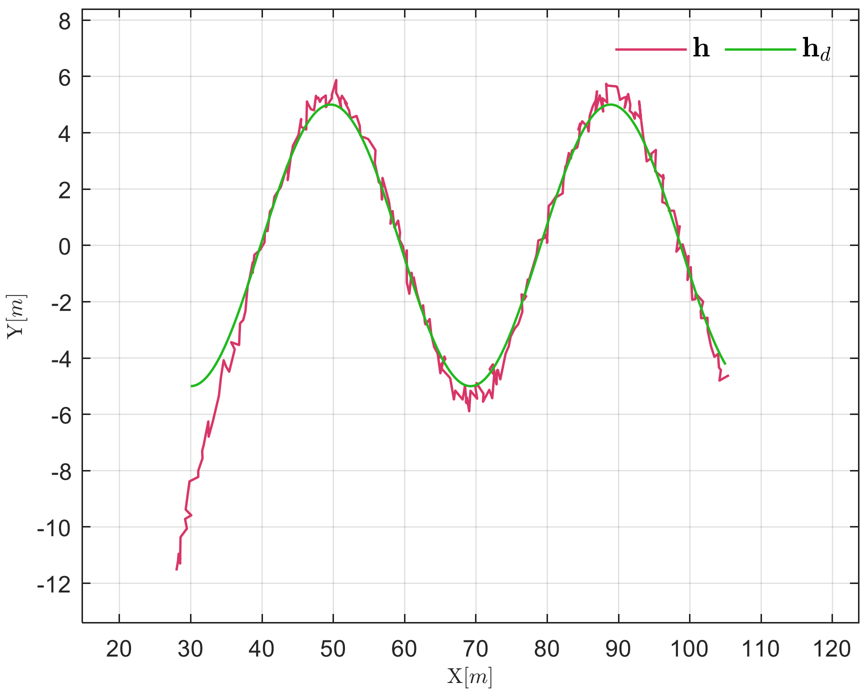

Figure 4. Definition of the trajectory

The control actions sent from Raspberry pi 3 b+ to the actuators versus the dynamic behavior performed by the vehicle is illustrated in figure 5.

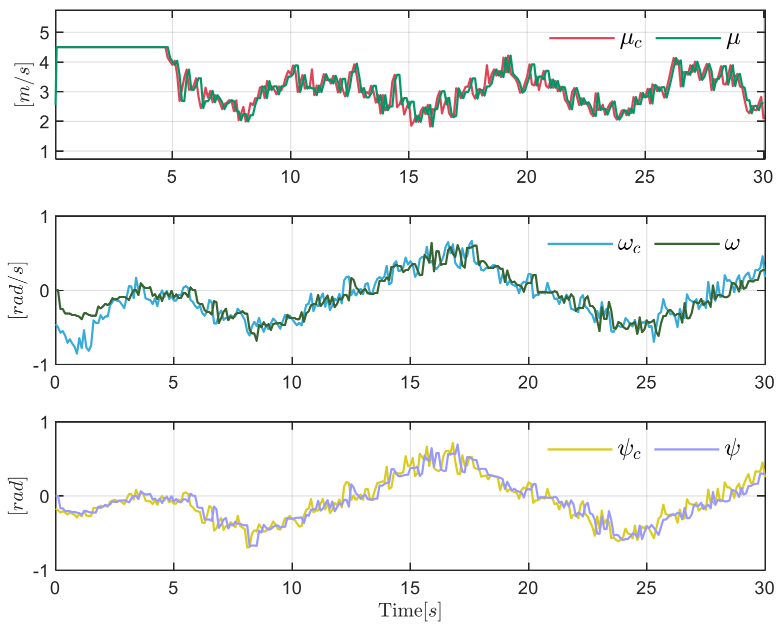

Figure 5. Control actions from Raspberry pi 3 b+ to the actuators versus the dynamic behavior performed by the vehicle.

In figure 5 three control actions are shown, among which is the desired linear speed μ_c versus what the vehicle μ is dynamically performing, then there is the desired angular speed ω_c versus what the vehicle is dynamically performing ω, and finally there is the angle ψ that the front wheels should take versus what the vehicle is actually performing ψ_c.

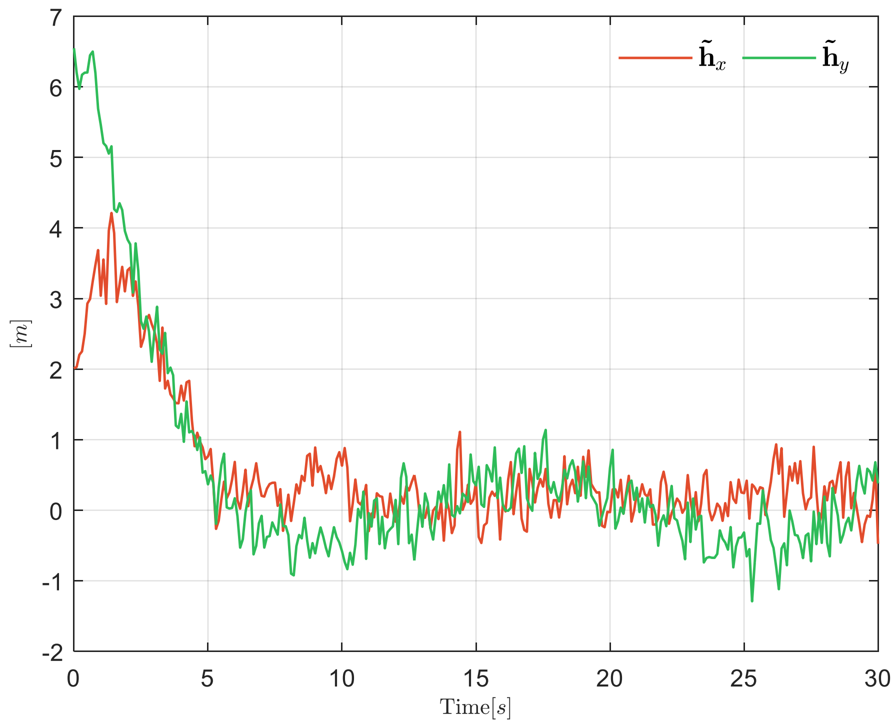

Figure 6. Errors of both latitude and longitude

Figure 6 shows the errors $\tilde{\mathbf{h}} = \begin{bmatrix} \tilde{\mathbf{h}}_x & \tilde{\mathbf{h}}_y \end{bmatrix}$ of both latitude and longitude, once these values have been transformed to Cartesian coordinates. It can be observed that at the beginning the error between the desired trajectory and the trajectory of the vehicle for the case of the axis and the axis has a value of 4 and 6 $[m]$ respectively, this is due to the fact that at an initial point the vehicle is positioned at a certain distance from the desired trajectory, then at a later point it is observed that the error oscillates between $\pm 1\ [m]$, this result is mainly due to the accuracy error generated by the GPS sensor and on the other hand by the dynamics of the MAZDA 6 vehicle itself.

In future research, experimental tests will be carried out with a new controller that on the one hand considers the dynamic compensations and on the other hand takes into account the avoidance of obstacles in the trajectory of the vehicle.

6. Conclusion

This article is the continuation of the proposal that has been previously validated in a 3D simulation program and now tested experimentally on a Mazda 6 vehicle instrumented with an electromechanical system that allows the guidance of a vehicle in a trajectory previously designed for autonomous driving applications. Errors between the vehicle position and the desired trajectory over time range between 1.5 meters of accuracy.

Authors' contribution: The authors contributed in all the research sections.

Financing: The authors fully financed the study.

Conflicts of interest: The authors declare that they have no conflicts of interest.

Referencias:

[1] M. Bersani *et al.*, "An integrated algorithm for ego-vehicle and obstacles state estimation for autonomous driving", *Rob. Auton. Syst.*, vol. 139, pp. 1–16, 2021, doi: https://doi.org/10.1016/j.robot.2020.103662.

[2] H. Atoui, O. Sename, E. Alcala, y V. Puig, "Parameter Varying Approach For A Combined (Kinematic + Dynamic) Model Of Autonomous Vehicles", *IFAC-PapersOnLine*, vol. 53, núm. 2, pp. 15071–15076, 2020, doi: https://doi.org/10.1016/j.ifacol.2020.12.2028.

[3] R. Kummerle, D. Hahnel, D. Dolgov, S. Thrun, y B. Wolfram, "Autonomous driving in a multi-level parking structure", *Robot. Autom.*, pp. 3395–3400, 2009, doi: 10.1109/ROBOT.2009.5152365.

[4] Z. Yu, Y. Hu, y J. Huang, "GPS/INS/Odometer/DR Integrated Navigation System Aided with Vehicular Dynamic Characteristics for Autonomous Vehicle Application", *IFAC-PapersOnLine*, vol. 51, núm. 31, pp. 936–942, 2018, doi: https://doi.org/10.1016/j.ifacol.2018.10.060.

[5] F. Castaño, G. Beruvides, A. Villalonga, y R. Haber, "Self-Tuning Method for Increased Obstacle Detection Reliability Based on Internet of Things LiDAR Sensor Models", *Sensors*, vol. 18, pp. 1–16, 2018, doi: https://doi.org/10.3390/s18051508.

[6] L. Wang, Y. Zhang, y J. Wang, "Map-Based Localization Method for Autonomous Vehicles Using 3D-LIDAR", *IFAC-PapersOnLine*, vol. 50, núm. 1, pp. 276–281, 2017, doi: https://doi.org/10.1016/j.ifacol.2017.08.046.

[7] G. Park, S. Choi, D. Hyun, y J. Lee, "Integrated observer approach using in-vehicle sensors and GPS for vehicle state estimation", *Mechatronics*, vol. 50, pp. 134–147, 2018, doi: https://doi.org/10.1016/j.mechatronics.2018.02.004.

[8] C. E. Tuncali, G. Fainekos, D. Prokhorov, y H. Ito, "Requirements-driven Test Generation for Autonomous Vehicles with Machine Learning Components", vol. 2, pp. 1–16, 2019, [En línea]. Disponible en: https://arxiv.org/pdf/1908.01094.pdf.

[9] X. Di y R. Shi, "A survey on autonomous vehicle control in the era of mixed-autonomy: From physics-based to AI-guided driving policy learning", *Transp. Res. Part C Emerg. Technol.*, vol. 125–40, pp. 1–40, 2021, doi: https://doi.org/10.1016/j.trc.2021.103008.

[10] Z. Ziye, L. Haiou, C. Huiyan, H. Jiaming, y G. Hongming, "Kinematics-aware model predictive control for autonomous high-speed tracked vehicles under the off-road conditions", *Mech. Syst. Signal Process.*, vol. 123, pp. 33–350, 2019, doi: https://doi.org/10.1016/j.ymssp.2019.01.005.

Author's review:

Danny José Zea Orellana. Ingeniero en Electrónica, Control y Redes Industriales en la Escuela Superior Politécnica de Chimborazo (ESPOCH). Máster Universitario en Ingeniería Electromecánica con mención en Mecatrónica de la Universidad Politécnica de Madrid. Trabajo de Fin de Máster en la línea de investigación: Sensores IoT en la Conducción Autónoma, realizado en el Consejo Superior de Investigaciones Científicas de Madrid. Participa como Docente Universitario y Docente Investigador en varios Proyectos de Investigación en la ESPOCH. Director del proyecto de investigación "Sensores IoT en vehículos para mejorar la seguridad vial". Actualmente cursa un PhD(c) en Automática y Robótica en la Universidad Politécnica de Madrid.